ACADEMIC PRESS

Available online at www.sciencedirect.com
SCIENCE DIRECT®

Journal of Catalysis 215 (2003) 254–263

JOURNAL OF CATALYSIS

www.elsevier.com/locate/jcat

Potential application of tungsten carbides as electrocatalysts III. Reactions of methanol, water, and hydrogen on Pt-modified C/W(111) surfaces

Ning Liu,[a] Kostantinos Kourtakis,[b] Juan C. Figueroa,[b] and Jingguang G. Chen [a,*]

[a] *Center for Catalytic Science and Technology, Department of Materials Science and Engineering, University of Delaware, Newark, DE 19716, USA*
[b] *DuPont Central Research and Development, Wilmington, DE 19880, USA*

Received 4 September 2002; revised 2 January 2003; accepted 7 January 2003

Abstract

The bonding and dissociation of methanol, water, and hydrogen on Pt-modified C/W(111) surfaces have been studied using high-resolution electron energy loss spectroscopy and temperature-programmed desorption. The decomposition pathways of methanol on C/W(111) are significantly modified by the presence of submonolayer coverages of Pt. For example, on the unmodified C/W(111) surface, the decomposition of methanol occurs via three pathways: (i) partial decomposition to produce carbon monoxide and hydrogen (∼ 31% selectivity), (ii) partial decomposition to form methane and atomic oxygen (∼ 14% selectivity), and (iii) complete decomposition to produce hydrogen, atomic carbon, and atomic oxygen (∼ 55% selectivity). In contrast, on the 0.6 monolayer (ML) Pt-modified C/W(111) surface, ∼ 49% of methanol partially dissociates to carbon monoxide and hydrogen, and the other ∼ 51% of methanol molecules undergo complete decomposition to hydrogen, atomic carbon, and atomic oxygen. The presence of submonolayer coverages of Pt prohibits the production of methane, which is an undesirable side product in direct methanol fuel cells. Furthermore, both the C/W(111) and the Pt-modified C/W(111) surfaces are active toward the dissociation of water. However, the amount of adsorbed water that undergoes dissociation is reduced from 0.18 H_2O per W atom on C/W(111) to 0.056 H_2O per W on the 0.6 ML Pt-modified C/W(111) surface. Finally, both C/W(111) and 0.6 ML Pt/C/W(111) surfaces are active toward the dissociation of hydrogen. These results demonstrated the possible synergistic effects by supporting low loading of Pt onto tungsten carbides for potential applications in methanol or hydrogen fuel cells.

Keywords: Fuel cells; Tungsten carbides; Pt-modified C/W(111)

1. Introduction

Due to the increasing concern over the diminishing supplies of fossil fuels and the environmental pollution from conventional engines, fuel cell technology has become one of the most promising solutions by converting chemical energy into electricity directly. There are six main fuel cell systems that are currently in various stages of development (alkaline, proton exchange membrane, phosphoric acid, molten carbonate, solid-state oxides, and direct methanol) [1]. At present, the direct methanol fuel cells (DMFC) and hydrogen fuel cells are among the leading fuel cell systems. The overall reactions involving the anodic oxidation of methanol and hydrogen can be described by

$$CH_3OH + H_2O \rightarrow CO_2 + 6H^+ + 6e^-, \quad (1)$$

$$H_2 \rightarrow 2H^+ + 2e^-. \quad (2)$$

Therefore, the desirable electrocatalysts in DMFC should be active toward the dissociation of both methanol and water, while those for hydrogen fuel cells should obviously be active toward the dissociation of hydrogen. At present, the most active catalysts for methanol and hydrogen fuel cells are primarily alloys of platinum, such as Pt–Ru [2–4] or Pt–Sn [3–10]. However, one of the disadvantages of using Pt-group metal electrocatalysts is the prohibitively high costs and limited supplies of these precious metals. Possible solutions are either to identify less expensive alternative electrocatalysts or to substantially reduce the loading of Pt-group metals.

* Corresponding author.
E-mail address: jgchen@udel.edu (J.G. Chen).

0021-9517/03/$ – see front matter
doi:10.1016/S0021-9517(03)00019-8

It is well known that carbides of early transition metals (Groups IV–VI) often have catalytic advantages over their parent metals in activity, selectivity, and resistance to poisoning [11,12]. Their catalytic activities are often similar to those of the more expensive Pt group (Pt, Pd, Ir, Rh, Ru) metals [11,12]. In previous studies, our group has demonstrated that carbide-modified V(110), Mo(110), and W(111) surfaces possess Pt-like properties in the transformation reactions of hydrocarbon molecules [13–21]. More recently, our group has started investigation of potential applications of tungsten carbides in direct methanol fuel cells. In two previous publications [22,23], we have reported the decomposition of methanol [22], as well as the co-adsorption of water and CO [23], on the C/W(111) surface. Our results indicate that the C/W(111) surface is very active toward the decomposition of methanol and water. However, we also observed that $\sim 14\%$ of adsorbed methanol undergoes partial decomposition to produce atomic oxygen and methane, with the latter being an undesirable side product for fuel cell applications.

The introduction of low concentrations of Pt-group metals onto a carbide support offers the possibility of reducing the loading of Pt-group metals by taking advantage of the Pt-like properties of the carbide support [24]. Our primary interest in studying the dissociation of methanol, water, and hydrogen on Pt-modified C/W(111) surfaces is to determine whether there is a synergistic effect by depositing submonolayer coverages of Pt onto the tungsten carbide surface. In the current paper, we have investigated the decomposition pathways of methanol and water on C/W(111) surfaces that were modified by submonolayer coverages of Pt. In addition, we will briefly compare the reactivities of Pt-modified C/W(111) to those of unmodified C/W(111) and of Pt-group metal surfaces to demonstrate the synergistic effect from using Pt-modified tungsten carbides as potential fuel cell electrocatalysts.

2. Experimental

The experiments were carried out in a multilevel UHV chamber, which was equipped with Auger electron spectroscopy (AES), temperature programmed desorption (TPD), low-energy electron diffraction (LEED), and high-resolution electron energy loss spectroscopy (HREELS). A detailed description about this UHV system and the preparation procedures for the C/W(111) surface have been published elsewhere [20]. The TPD data were collected using a Teknivent data acquisition system, which enabled us to collect up to 12 masses simultaneously. A linear heating rate of 3 K s^{-1} was used for all experiments. The beam energy in the HREELS measurements was approximately 6 eV with a typical resolution between 37 and 45 cm^{-1}.

CH_3OH (99+%) and CH_3OD (99+%) were purchased from Aldrich Chemical Company. CD_3OH (99.5%) was purchased from Cambridge Isotope Laboratories. All chemicals were purified by successive freeze–pump–thaw cycles and their purity was verified in-situ by mass spectrometry. All chemicals were introduced into the vacuum chamber via leak valves and the gas pressures were measured by uncorrected ion gauges.

The deposition of submonolayer coverages of Pt was achieved by heating Pt wire (0.127 mm in diameter, 99.9% from Alfa Aesar) that was wrapped tightly on W heating wires [25]. The preparation of Pt-modified C/W(111) and the estimation of Pt coverage have been described elsewhere [25]. Briefly, the coverage of Pt was calculated based on the attenuation of the Auger W(182 eV) peak after the deposition of Pt [25]. The C/W(111) surfaces were prepared by repeating cycles of exposing W(111) to 2.2 L ethylene at 90 K followed by flashing to 1200 K. After three to four cycles, the C/W(111) surface is obtained and characterized by a $(\sqrt{3} \times \sqrt{3})$R30° LEED pattern with an atomic C/W(111) ratio of approximately 0.55, based on the standard AES sensitivity factors [26]. Upon the deposition of submonolayer Pt the surface retains the $(\sqrt{3} \times \sqrt{3})$R30° pattern. We did not observe the (2×1) LEED pattern that was reported upon the deposition of near-monolayer coverage of Pt on a clean W(111) surface [27–29]. The absence of the (2×1) LEED pattern strongly suggests that the Pt overlayer does not form the ordered Pt(211) nanofacets that have been detected on clean W(111) [27–29]. However, in the current study the LEED and AES results alone are not sufficient to conclude the exact morphology/structure of the submonolayer Pt on C/W(111). We are planning to characterize the structural properties of the Pt/C/W(111) surfaces using scanning tunneling microscopy.

3. Results and interpretation

3.1. TPD results

3.1.1. Decomposition of methanol

Fig. 1 shows the TPD spectra of mass 2 amu following 1.0 L exposure of methanol on C/W(111) and two Pt-modified C/W(111) surfaces. The Pt coverages on the two Pt-modified C/W(111) surfaces correspond to 0.3 and 0.6 ML Pt, respectively. There is a broad hydrogen peak centered at around 385 K, with an asymmetric shoulder at 458 K, on all three surfaces. The areas of the hydrogen TPD peaks are related to the degree of methanol dissociation on these three surfaces, as will be discussed later. The peak center and lineshape of the H_2 TPD from 1.0 L CH_3OH on C/W(111) are slightly different from those reported earlier [22], which may be due to differences in the pumping speed and UHV base pressures during the two sets of TPD measurements.

Fig. 2 shows the TPD spectra of masses 32, 28, 15, and 16 amu following 1.0 L exposure of methanol on C/W(111) and three Pt-modified C/W(111) surfaces. The three Pt-

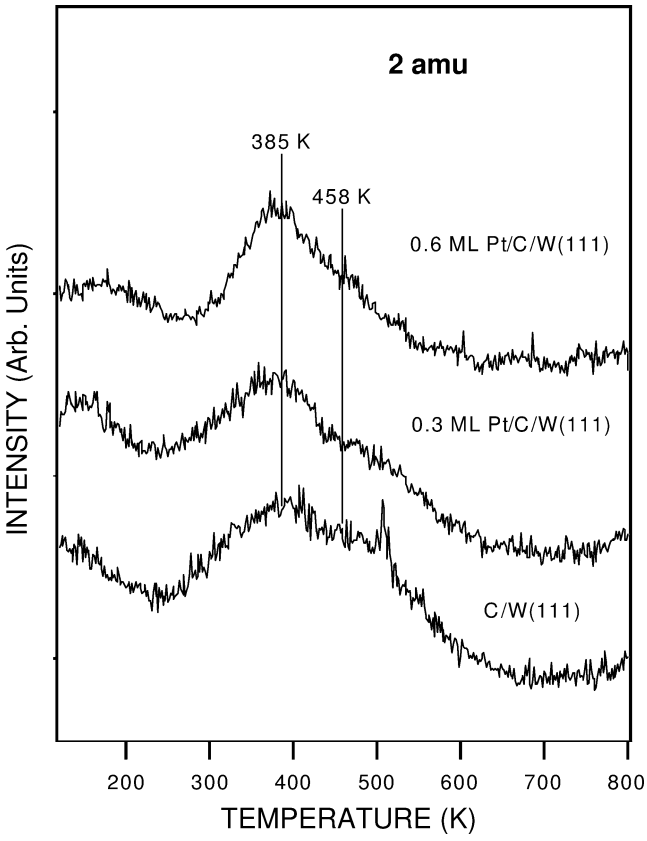

Fig. 1. TPD spectra of hydrogen (2 amu) after exposing C/W(111), 0.3 ML Pt/C/W(111), and 0.6 ML Pt/C/W(111) to 1.0 L CH_3OH at 90 K.

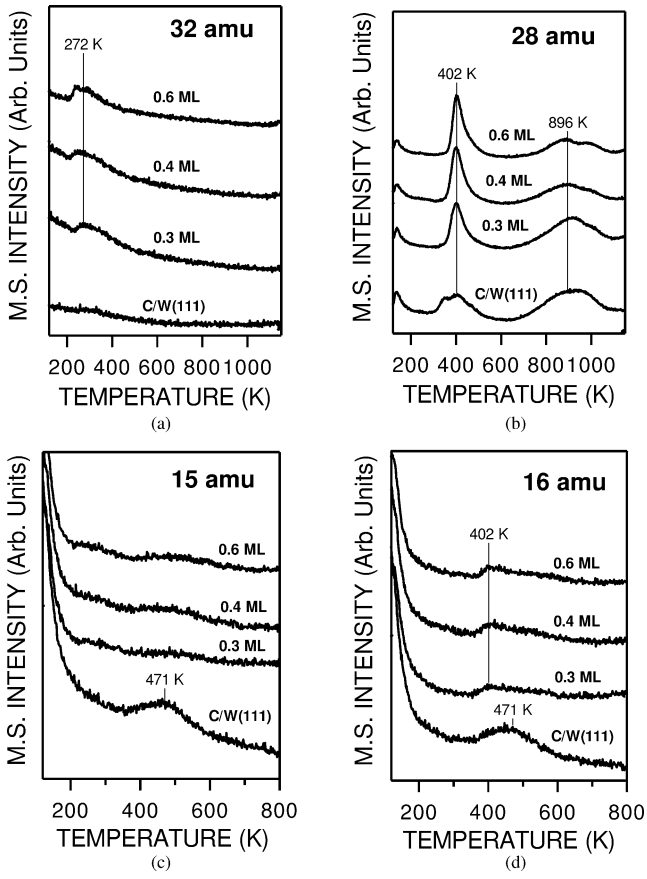

Fig. 2. TPD spectra of 32, 28, 16, and 15 amu masses after exposing C/W(111), 0.3 ML Pt/C/W(111), 0.4 ML Pt/C/W(111), and 0.6 ML Pt/C/W(111) to 1.0 L CH_3OH at 90 K.

modified C/W(111) surfaces correspond to Pt coverages of 0.3, 0.4, and 0.6 ML. In Fig. 2a, methanol (32 amu) desorbs molecularly around 272 K. In Fig. 2b, there are two features of carbon monoxide (28 amu), one sharp feature at 402 K, and the other is a broad peak centered at around 896 K. The latter CO desorption peak is due to the recombination of atomic carbon and oxygen [22,23]. Because mass 15 amu is a major cracking pattern of methane (16 amu), Figs. 2c and 2d show the TPD spectra of both mass 15 amu and methane (16 amu) to illustrate the formation of methane. On the C/W(111) surface, a peak at 471 K is observed in TPD spectra of both mass 15 and mass 16 amu, suggesting that the methane (16 amu) is a reaction product, instead of being from the cracking pattern of CO (28 amu). On the three Pt-modified C/W(111) surfaces, the weak peaks of mass 16 amu are observed around 402 K, with the absence of mass 15 amu and the presence of mass 28 amu at the same temperature. This indicates that the feature at 402 K is from the cracking pattern of CO (28 amu) instead of methane (16 amu) on the three Pt-modified C/W(111) surfaces.

3.1.2. Dissociation of water

Fig. 3 shows the TPD spectra of mass 18, mass 2, and mass 28 amu obtained following 1.0 L exposure of water on C/W(111) and 0.6 ML Pt/C/W(111). On both surfaces, H_2O desorbs molecularly at 163 and 153 K and the broad hydrogen peaks are detected around 174 and 166 K, respectively. On C/W(111), there are also weak shoulders at around 295 and 377 K, as shown in previous studies [23]. On the 0.6 ML Pt/C/W(111) surface, CO desorbs at 826 K. On C/W(111), the broad feature of CO desorption is observed around 920 K. As described earlier, these high-temperature CO features are produced by recombination of atomic carbon and oxygen. Overall, the TPD results in Fig. 3 indicate that both C/W(111) and 0.6 ML Pt/C/W(111) surfaces are active toward the dissociation of water, although the degree of dissociation is different as will be quantified later.

3.1.3. Dissociation of hydrogen

TPD results following the dissociation of hydrogen on C/W(111) and 0.3 ML Pt/C/W(111) surfaces are compared in Fig. 4. In these experiments the surfaces were first exposed to 0.5 L of H_2 and then to 50 L of D_2 at 90 K. TPD measurements were then performed to detect one of the reaction products, HD (3 amu). As compared in Fig. 4, the HD product desorbs from the surfaces over a very broad range of temperatures, with the peak center appearing at $\sim$ 311 K on C/W(111) and at $\sim$ 297 K on 0.3 ML Pt/C/W(111). The detection of the HD product

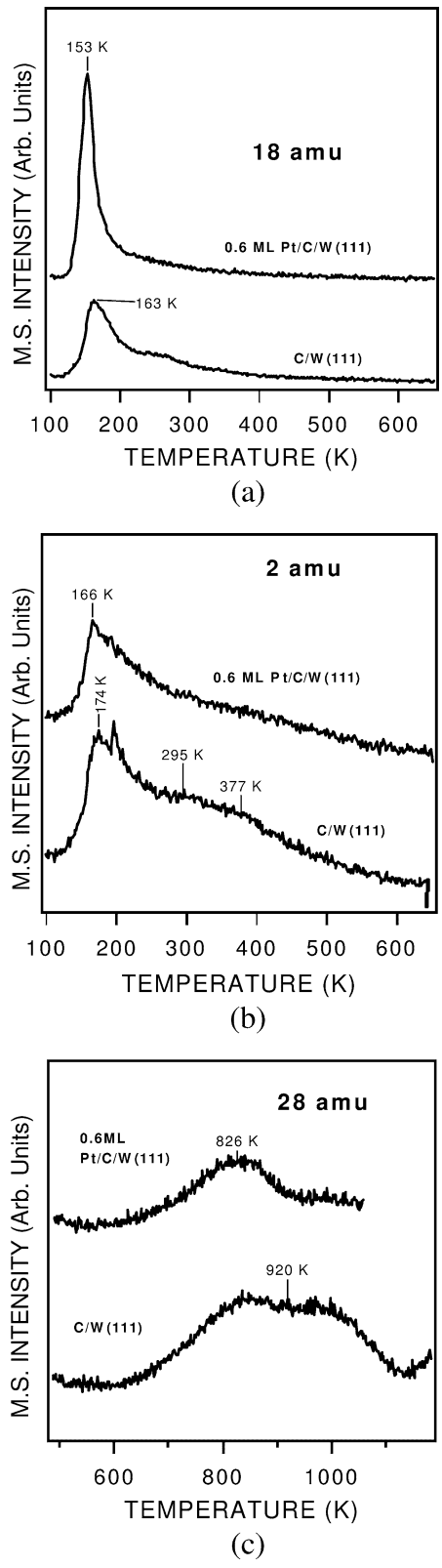

Fig. 3. TPD spectra of water (18 amu), hydrogen (2 amu), and carbon monoxide (28 amu) after exposing C/W(111) and 0.6 ML Pt/C/W(111) to 1.0 L H_2O at 90 K.

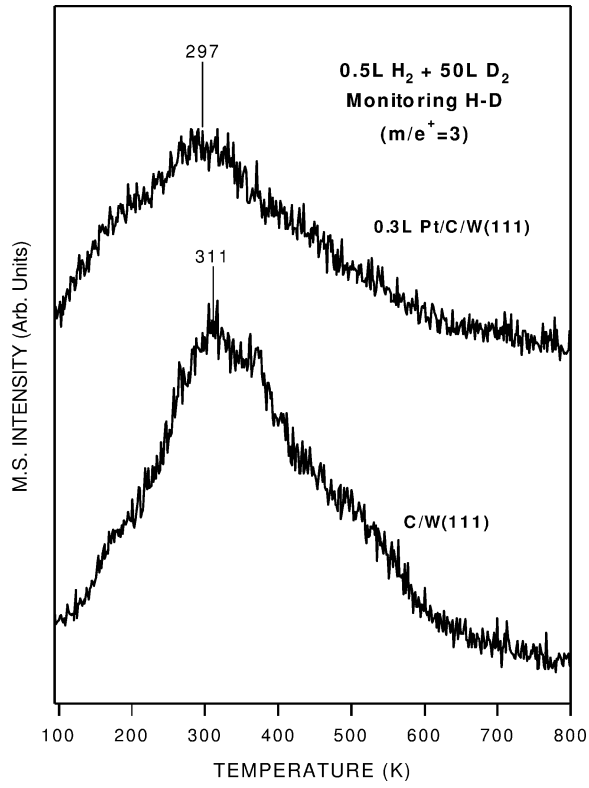

Fig. 4. TPD spectra of HD (3 amu) after exposing C/W(111) and 0.3 ML Pt/C/W(111) to 0.5 L H_2 and 50 L D_2 at 90 K.

from the two surfaces indicates that C/W(111) and 0.3 ML Pt/C/W(111) surface are both active toward the dissociation of hydrogen, although the HD yield is higher on the unmodified C/W(111) surface.

3.2. HREELS results

We have performed HREELS measurements to characterize the surface intermediates of methanol and water on the submonolayer Pt/C/W(111) surfaces. Figs. 5–7 show the thermal behavior of CH_3OH, CH_3OD, and CD_3OH on Pt/C/W(111), respectively. For comparison, Fig. 8 shows the thermal behavior of CH_3OD and CD_3OH on the unmodified C/W(111) surface. Finally, Fig. 9 shows the dissociation pathway of H_2O on 0.6 ML Pt/C/W(111). To monitor thermal properties of adsorbed methanol and water, each of the surfaces was flashed to the indicated temperatures and cooled back to 90 K for HREELS measurements. The vibrational assignments are summarized in Tables 1–3 for methanol, methoxy species, and water, respectively. The different temperatures, 90, 230, 330, 450, and 600 K, were chosen primarily based on the TPD results described earlier.

3.2.1. Methanol on Pt/C/W(111)

Fig. 5 shows the HREELS spectra of the thermal behavior of 1.0 L CH_3OH on the 0.6 ML Pt/C/W(111) surface. To assign the vibrational features observed in Fig. 5, HREELS

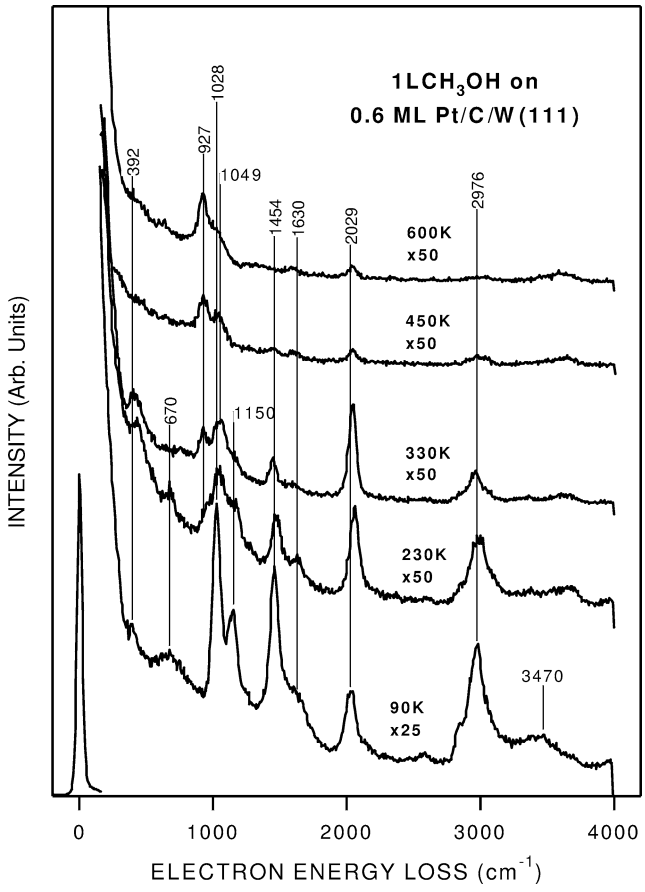

Fig. 5. HREEL spectra monitoring thermal properties of 1.0 L CH_3OH adsorbed on 0.6 ML Pt/C/W(111).

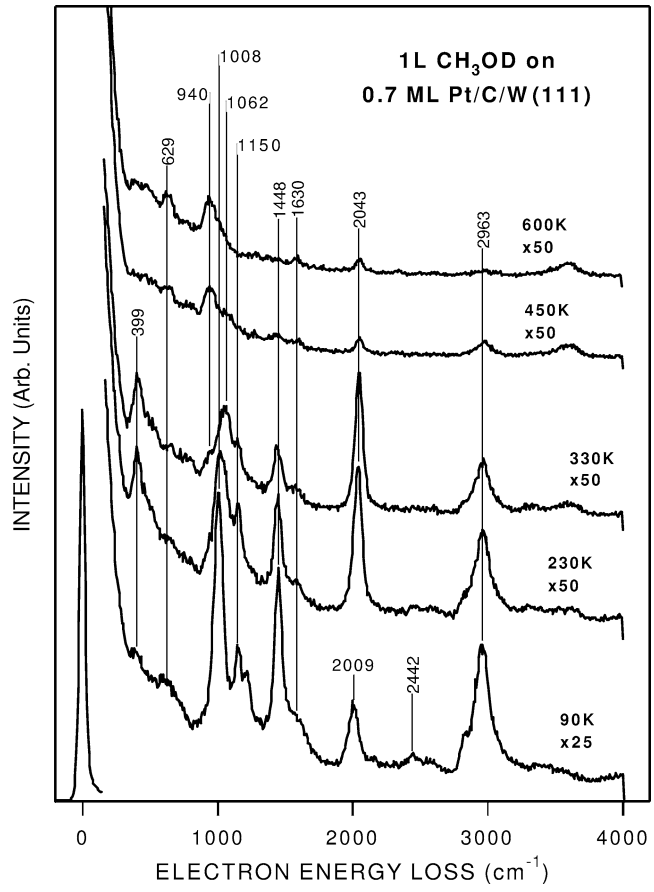

Fig. 6. HREEL spectra monitoring thermal properties of 1.0 L CH_3OD adsorbed on 0.7 ML Pt/C/W(111).

spectra of the thermal behavior of CH_3OD and CD_3OH on Pt/C/W(111) surfaces are compared in Figs. 6 and 7. As summarized in Table 1, based on the characteristic frequency shifts upon partial deuteration, and by comparing with the frequencies of the solid phase CH_3OH, CH_3OD, and CD_3OH [30], the spectra observed at 90 K can be assigned to molecularly adsorbed methanol. In the spectrum of CD_3OH at 90 K (Fig. 7), the detection of the relatively weak $\delta(CH_3)$ mode at 1414 cm^{-1} and $\nu(CH_3)$ mode at 2990 cm^{-1} is likely contributed by the residue CH_3OH in the gas-handling system.

After heating the surface to 230 K, the most important spectroscopic change is the disappearance of the ν(OH) and ν(OD) modes, at 3470 cm^{-1} for CH_3OH, at 3321 cm^{-1} for CD_3OH, and at 2442 cm^{-1} for CH_3OD. The scission of the O–H or O–D bond indicates the formation of the methoxy intermediate at 230 K. Vibrational characterization of the methoxy species has been the subject of many detailed studies and will not be discussed in detail here. In Table 2 we compare the different modes of CH_3O and CD_3O to those reported on Al(111) [31]. The vibrational assignment is very straightforward. For example, the observation of very similar spectra, from the scission of CH_3OH and CH_3OD, confirms the formation of the methoxy species. Furthermore, based on the characteristic frequency shifts upon partial deuteration, the ν_H/ν_D ratios of the methyl vibrational features are ~ 1.3 and the ν_D/ν_D ratio of the ν(C–O) mode is ~ 1, which are similar to those reported on Al(111) and on many other surfaces.

After heating to 330 K, all the vibrational features of methoxy remain on the surface, although the intensities of these features decrease significantly. Such decreases indicate that a significant fraction of the methoxy groups undergo decomposition at the temperature range between 230 and 330 K. After 450 K, all modes related to the surface methoxy species disappear and only the broad, asymmetric feature centered at 913–940 cm^{-1} is observed.

As shown in the top spectra in Figs. 5–7, after heating to 600 K only one asymmetric feature remains in the frequency range of 913–940 cm^{-1}, with a shoulder at approximately 1001–1060 cm^{-1}. We tentatively assign these features to the contribution of the ν(M–O) and ν(M–C) modes, based primarily on three observations: (i) The frequencies of these features do not shift substantially upon the partial deuteration by comparing CH_3OH to CD_3OH and CH_3OD, which rules out the possibility of vibrational modes involving any CH_x groups. (ii) The intensity of the main feature at 913–940 cm^{-1} increases with the complete

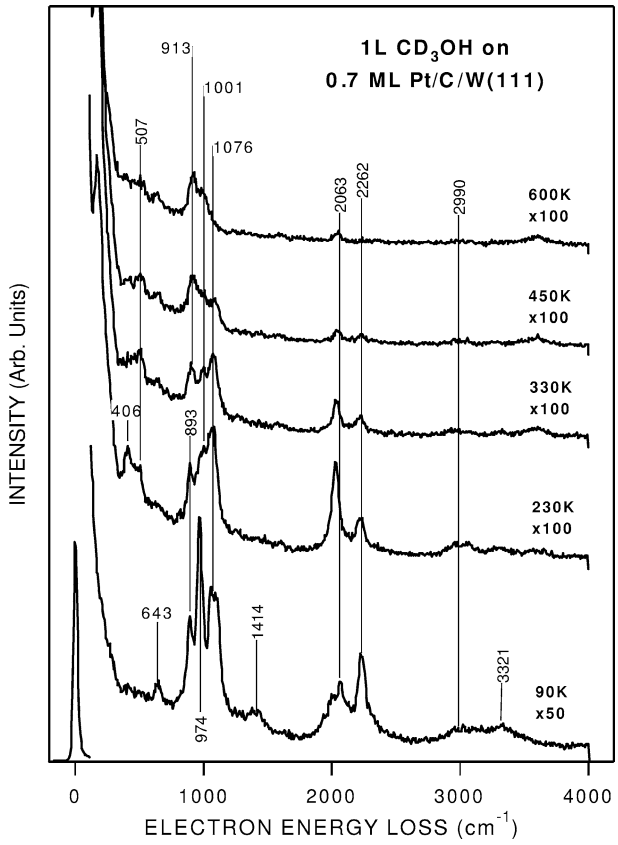

Fig. 7. HREEL spectra monitoring thermal properties of 1.0 L CD_3OH adsorbed on 0.7 ML Pt/C/W(111).

decomposition of methanol, suggesting that the vibrational feature is related to the surface species produced from the complete dissociation, i.e., atomic carbon and atomic oxygen. (iii) AES measurements reveal the presence of carbon and oxygen on all three 600 K surfaces in Figs. 5–7.

In addition to the vibrational modes of methoxy, Figs. 5–7 show two other vibrational features. The mode at between 2029 and 2063 cm^{-1} is due to the accumulation of background CO on the surface during the data acquisition (about 30 min per spectrum). In addition, a relatively weak peak is observed for CH_3OH and CH_3OD at ~ 1630 cm^{-1}. Although this frequency is typically related to the ν(C=C) mode of unsaturated hydrocarbons, the absence of this mode in the CD_3OH spectra rules out the possibility of the formation of any surface intermediates with C=C bond. At present we do not know the exact origin of the ~ 1630 cm^{-1} mode.

Finally, in order to highlight the differences between the decomposition of methanol on Pt/C/W(111) and on unmodified C/W(111) surfaces, Fig. 8 compares the decomposition of CH_3OD and CD_3OH on the C/W(111) surface. By comparing the thermal behavior in Fig. 8 with the corresponding isotopes in Figs. 6 and 7, it is clear that the decomposition pathways of methanol are different on the two types of surfaces in two important aspects: (i) Comparing to Pt/C/W(111), the unmodified C/W(111) surface is more active toward the scission of the O–H (O–D) bonds and the formation of the methoxy intermediate, as indicated by the absence of the ν(O–H) or ν(O–D) mode at 90 K [22]. In this regard the presence of submonolayer coverages of Pt reduces the activity of the C/W(111) surface toward the dissociation of the O–H (O–D) bonds. (ii) On the other hand, the presence of submonolayer coverages of Pt enhances the subsequent decomposition of methoxy, as indicated by the significant decrease in the intensities of the methoxy vibrational modes on Pt/C/W(111) between 230 and 330 K in Figs. 6 and 7. In contrast, the vibrational intensities of methoxy on unmodified C/W(111) actually show an increase from 230 to 330 K. As described in detail in a previous paper [22], this increase is related to a thermally induced change in the orientation of the methoxy species on the C/W(111) surface.

3.2.2. Water on 0.6 ML Pt/C/W(111)

Fig. 9 shows HREELS spectra of the thermal decomposition of 1.0 L H_2O on the 0.6 ML Pt/C/W(111) surface. Compared to vibrational features of the solid-state H_2O [32], the vibrational features of H_2O on 0.6 ML Pt/C/W(111) are assigned in Table 3. The observation of the ν(OH) mode of isolated OH groups at 3687 cm^{-1} indicates that a fraction of H_2O molecules dissociates on the surface even at 90 K. The characteristic vibrational frequencies related to the molecular H_2O include the δ(HOH) mode at 1637 cm^{-1}, ν(OH) H_2O mode at 3477 cm^{-1}, hindered translation mode at 257 cm^{-1}, and hindered rotations mode at 683 cm^{-1}. These molecular H_2O modes almost completely disappear after heating the surface to 230 K, indicating that most of H_2O molecules dissociate by 230 K. The frequency of the ν(OH) mode of surface hydroxyl shifts from 3687 to 3599 cm^{-1}. The features at 2956 and 1251 cm^{-1} are assigned to the ν(C–H) and δ(C–H) modes, respectively, of adsorbed CH_x species. The surface CH_x fragments are either produced via the reaction of hydrogen atoms (from the complete dissociation of H_2O) with the atomic carbon from 0.6 ML Pt/C/W(111) surface, or due to the accumulation of background hydrocarbons during the data acquisition. The presence of the ν(CO) mode at 2023 cm^{-1} is due to accumulation of background CO during the HREELS measurements. Finally, the relatively weak features at 1583 and 3267 cm^{-1} are tentatively assigned to the δ(HOH) and ν(OH) modes, respectively, of hydrogen-bonded H_2O on the surface.

After heating the surface to 330 K, a new vibrational feature appears at 900 cm^{-1}. After heating to 450 K, almost all of the surface hydroxyl groups have disappeared, and the intensity of the 900 cm^{-1} feature further increases. AES measurements reveal the presence of oxygen and carbon on the 0.6 ML Pt/C/W(111) surface after the dissociation of H_2O at 450 K. Similar to the vibrational assignment after the dissociation of methanol on Pt-modified C/W(111) surfaces, we assign the 900 cm^{-1} feature as the mixture of the ν(M–O) and ν(M–C) modes on the Pt/C/W(111) surface.

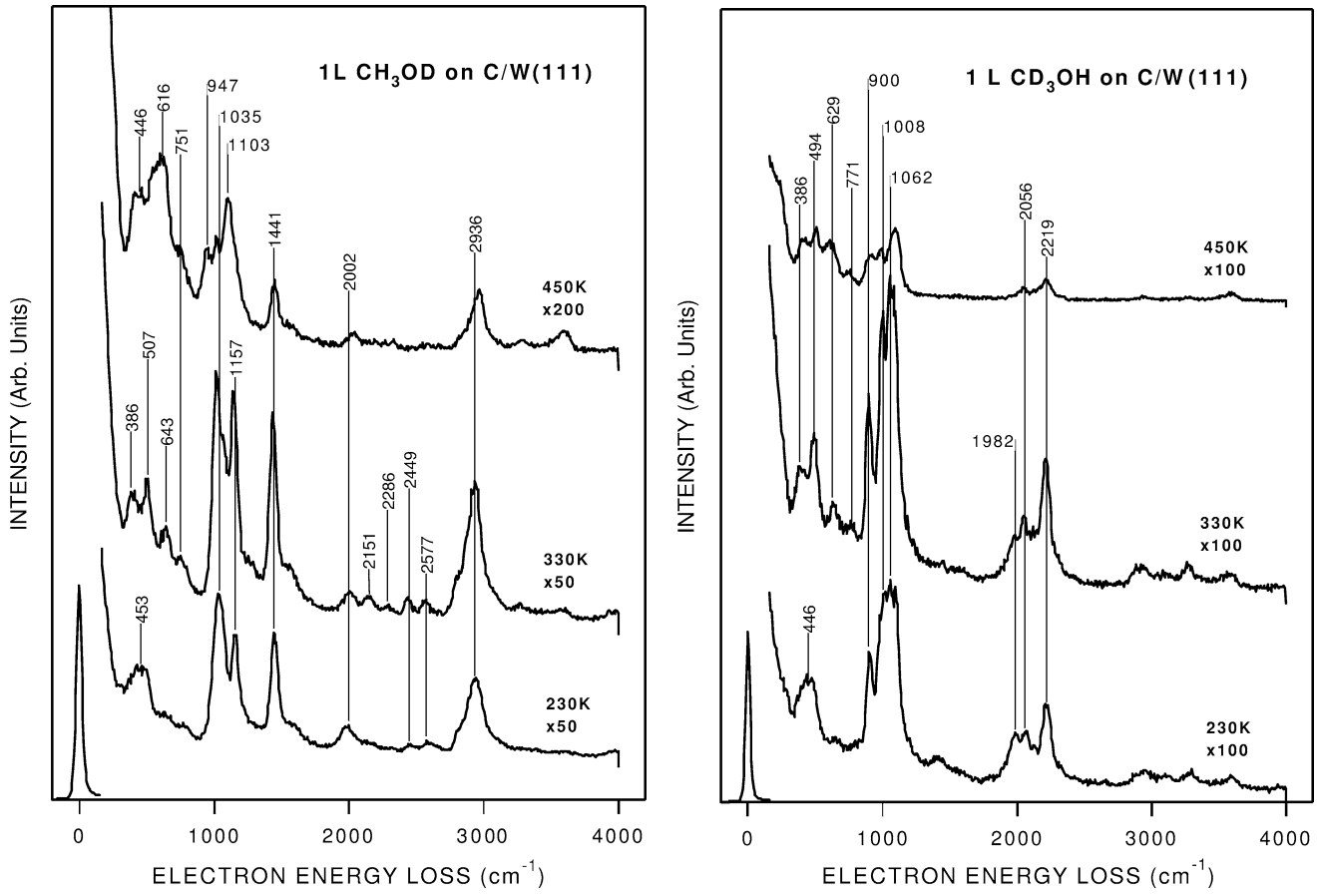

Fig. 8. HREEL spectra monitoring thermal properties of 1.0 L CH_3OD (left panel) and 1.0 L CD_3OH (right panel) adsorbed on unmodified C/W(111) surfaces.

4. Discussion

4.1. Product yields of CH_3OH on 0.6 ML Pt/C/W(111)

To facilitate calculation of the product yields of CH_3OH on 0.6 ML Pt/C/W(111), we will first briefly describe the product yields on C/W(111). As described in our previous paper on the C/W(111) surface, CO, CH_4, and H_2 are the only gas-phase products from methanol [22]. Additionally, there are two CO desorption peaks at around 402 and 896 K, with the latter being from the recombination of atomic carbon and oxygen. Therefore, the decomposition of methanol occurs via three reaction pathways, as shown in Eqs. (3)–(5). The symbols a, b, and c represent the number of methanol (methanol molecules per W atom) involved in each of the reaction pathways on C/W(111):

$$\underset{a}{CH_3OH} \rightarrow \underset{a}{CO} + \underset{2b}{2H_2}, \tag{3}$$

$$\underset{b}{CH_3OH} \rightarrow \underset{b}{C} + \underset{b}{O} + \underset{2b}{2H_2}, \tag{4}$$

$$\underset{c}{CH_3OH} \rightarrow \underset{c}{CH_4} + \underset{c}{O}. \tag{5}$$

As reported in our previous paper [22], we have determined that the values of a, b, and c are 0.087, 0.155, and 0.038 methanol molecules per W atom, respectively. From these values we estimated that $\sim 31\%$ methanol molecules decompose to produce CO and H_2, $\sim 55\%$ methanol molecules undergo complete decomposition to atomic carbon, atomic oxygen and H_2, and the other $\sim 14\%$ of methanol molecules decompose to produce gas-phase methane and atomic oxygen.

As compared in the TPD results (Fig. 2), CO, and H_2 are the only gas-phase products from the dissociation of methanol on the 0.6 ML Pt/C/W(111) surface. There are again two CO desorption features, observed at around 402 and 896 K. However, methane is not detected from the Pt/C/W(111) surfaces. The two decomposition pathways of methanol on Pt/C/W(111) are shown in Eqs. (6) and (7). The symbols d and e represent the number of methanol involved in each of the reaction pathways:

$$\underset{d}{CH_3OH} \rightarrow \underset{d}{CO} + \underset{2d}{2H_2}, \tag{6}$$

$$\underset{e}{CH_3OH} \rightarrow \underset{e}{C} + \underset{e}{O} + \underset{2e}{2H_2}. \tag{7}$$

By comparing the TPD area of the recombinative CO peak (873K) from 1.0 L methanol on 0.6 ML Pt/C/W(111)

Table 1
Vibrational assignments (cm^{-1}) of solid phase CH_3OH, CH_3OD, and CD_3OH and those observed for methanol adsorption on Pt/C/W(111) at 90 K

Mode	Methanol(s) [30]			Methanol on Pt/C/W(111)		
	CH_3OH	CH_3OD	CD_3OH	CH_3OH	CH_3OD	CD_3OH
ν(M–O)	–	–	–	670	629	643
δ(OH)	730	535	708	–	–	–
ν(C–O)	1032	1032	983	1028	1008	974
$\gamma(CH_3)$	1124	1158	895	1150	1150	893
$\delta(CH_3)$	1452	1470	1122	1454	1448	1076
$\nu s(CH_3)$	2828	2835	2075	–	–	–
$\nu as(CH_3)$	2951	2957	2213	2976	2963	2262
ν(OH)	3225	2400	3195	3470	2442	3321

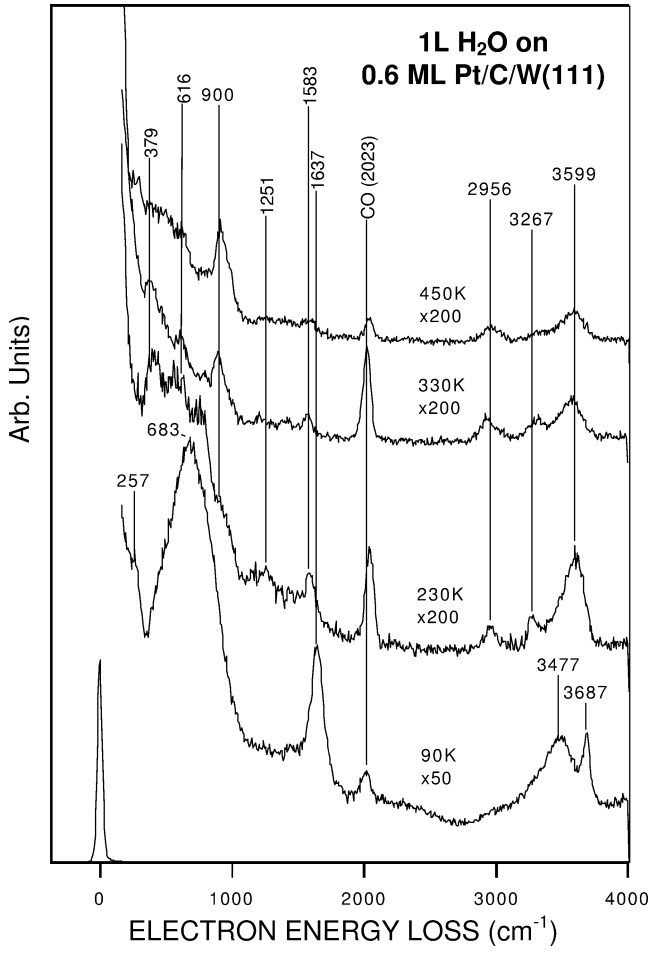

Fig. 9. HREEL spectra monitoring thermal properties of 1.0 L H_2O adsorbed on 0.6 ML Pt/C/W(111).

to that on C/W(111), a value of 0.59 is obtained. This leads to the following relationship:

$$e/b = 0.59. \tag{8}$$

Furthermore, by comparing the TPD area of H_2 from 1 L methanol on 0.6 ML Pt/C/W(111) to that from 1 L methanol on C/W(111), the ratio of 0.73 is obtained. It leads to the relationship

$$(2d + 2e)/(2a + 2b) = 0.73. \tag{9}$$

After solving Eqs. (8) and (9), the values of d and e are determined to be 0.091 and 0.086 methanol molecules per W atom, respectively. Therefore, we can estimate that $\sim 49\%$ of methanol molecules decompose to CO and hydrogen and the other $\sim 51\%$ methanol molecules decompose to atomic carbon, atomic oxygen, and H_2. Furthermore, from these values we can also estimate the overall surface reactivity toward the dissociation of methanol. On 0.6 ML Pt/C/W(111) the surface activity is estimated to be 0.177 methanol per W atom (values of $d + e$), which is lower than the surface activity of 0.280 methanol per W atom (values of $a + b + c$) on the unmodified C/W(111) surface.

4.2. Product yields of H_2O

As shown in Eqs. (10) and (11), H_2O dissociates to produce hydrogen and atomic oxygen on both C/W(111) and 0.6 ML Pt/C/W(111) surfaces. The atomic oxygen then recombines with the carbon atoms of C/W(111) or Pt/C/W(111) to produce gas-phase CO at $T \gtrsim 800$ K:

$$H_2O \rightarrow O(a) + H_2 \tag{10}$$

$$O(a) + C/W(111) \overset{\gtrsim 800\ K}{\rightarrow} CO(g). \tag{11}$$

By comparing TPD areas of CO (> 800 K) from 1.0 L H_2O on 0.6 ML Pt/C/W(111) to that on C/W(111), a ratio of 0.31 is obtained, which leads to the relationship

$$\frac{\text{CO from } H_2O/Pt/C/W(111)}{\text{CO from } H_2O/C/W(111)} = 0.31. \tag{12}$$

In a previous paper [23] we have determined that 0.18 water molecules per W atom undergo complete dissociation on C/W(111). Therefore the TPD area of CO (> 800 K) from 1.0 L H_2O on C/W(111) in Fig. 3 corresponds to 0.18 CO per W atom. By solving Eq. 12, the TPD area of CO (> 800 K) from 1.0 L H_2O on 0.6 ML Pt/C/W(111) corresponds to 0.056 [0.18×0.31] CO molecules per W atom, which in turn indicates that the number of H_2O undergoing dissociation on the 0.6 ML Pt/C/W(111) surface is 0.056 water molecule per W atom.

Table 2
Vibrational assignments (cm^{-1}) for methoxy species of CH_3O and CD_3O on Al(111) and Pt/C/W(111)

Mode	Methoxy on Al(111) [31]			Methoxy on Pt/C/W(111)			
	CH_3O	CD_3O	ν_H/ν_D	CH_3O (from CH_3OH)	CD_3O (from CD_3OH)	ν_H/ν_D	CH_3O (from CH_3OD)
ν(C–O)	1025	985	1.04	1049	1001	1.05	1062
$\gamma(CH_3)$	1170	–	–	1150	893	1.29	1150
$\delta(CH_3)$	1475	1080	1.37	1454	1076	1.35	1448
$\nu s(CH_3)$	–	2065	–	–	–	–	–
$\nu as(CH_3)$	2970	2235	1.33	2976	2262	1.32	2963

Table 3
Vibrational frequencies (cm^{-1}) of solid phase H_2O and that observed for H_2O on 0.6 ML Pt/C/W(111) at 90 K

Mode	H_2O(s) [32]	H_2O on 0.6 ML Pt/C/W(111)
Hindered translation	180–300	257
Hindered rotations	400, 1050	683
δ(HOH)	1595	1583
		1637
ν(OH)	3220	3267
ν(OH)	3400	3477

4.3. Dissociation of hydrogen

The quantification of the HD product yield is complicated by the very broad desorption peak, as shown in Fig. 4. It would also require a detailed mass balance of the other two gas-phase reaction products, H_2 and D_2, from C/W(111) and Pt/C/W(111) surfaces. In the current study we did not attempt to quantify the yield of HD. However, the qualitative conclusion from the TPD results in Fig. 4 clearly confirms that both C/W(111) and Pt/C/W(111) surfaces are active toward the dissociation of hydrogen, although the HD yield on Pt/C/W(111) is lower than that on C/W(111) under identical experimental conditions.

4.4. Comparison of Pt/C/W(111) with C/W(111) and Pt surfaces

The adsorption of methanol on metal surfaces has been investigated extensively using surface science techniques under UHV conditions [31,33–42]. On Pt(111), methanol undergoes reversible molecular adsorption and desorption [33,34]. On oxygen-modified Pt(111) a fraction of adsorbed methanol dissociates to produce methoxy species, which further decomposes to CO and H_2, and a small fraction of the products is further oxidized to CO_2 and H_2O by the oxygen adatoms [35–38]. The interaction of water on metal surfaces has also been extensively studied. A detailed review of water on transition metals surfaces has been discussed by Thiel and Madey [43]. For example, on Pt surfaces, including (100) [44], (111) [45,46] surfaces, water adsorbs molecularly. It is proposed that water tends to form three-dimensional hydrogen-bonded clusters, even at fractional monolayer coverages, because the strength of the attractive interaction between two water molecules is comparable to that of the substrate H_2O bond [43]. As a result, the Pt surfaces are relatively inert toward the dissociation of water.

Overall, the clean surfaces of Pt are essentially inert toward the dissociation of methanol or water under UHV conditions. In contrast, as reported in the current study, the submonolayer Pt/C/W(111) surfaces are active toward the decomposition of both molecules. Furthermore, the presence of submonolayer coverages of Pt enhances the decomposition of methoxy in the temperature range of 230–330 K. This enhanced activity might be attributed to the higher activity of Pt toward the dissociation of the C–H bonds of methoxy, which should in turn be responsible for the elimination of the reaction pathway for the formation of the undesirable methane product on C/W(111). Therefore, there appears to be a synergistic effect by modifying the tungsten carbide surfaces with submonolayer coverages of Pt.

The origin of the observed synergistic effect can be attributed to the different chemical properties of C/W(111) and Pt surfaces. As demonstrated in previous studies of the dissociation of methanol on Group VI metals, Cr(110) [47], Mo(110) [48], W(110) [49], and W(111) [22], these early transition metals and the corresponding carbide-modified surfaces [22,48,49] are very active toward the dissociation of the O–H bond of methanol. This is confirmed by the formation of the methoxy species at the liquid nitrogen temperature, as indicated in Refs. [22,47–49]. In contrast, the Pt surfaces are nearly inert toward the cleavage of the O–H bond of methanol, leading to the reversible adsorption and desorption of methanol molecules from Pt surfaces [33–42].

However, the clean and carbide-modified Mo and W surfaces are relatively inert toward the subsequent decomposition of the methoxy species, which remain intact in the temperature range between 80 and 330 K (see Fig. 8 and Refs. [48,49]). The detection of the methane product at higher temperatures also suggests that carbide-modified surfaces are relatively inert toward the dissociation of the C–H bonds of methoxy. In contrast, it is well known that Pt surfaces are very active in the cleavage of C–H bonds of adsorbed hydrocarbon species [50]. One well-documented example is the facile production of the CH_2CH and CH_3C species from the dissociation of ethylene on Pt(111) [50].

Therefore, the combination of submonolayer Pt on C/W(111) leads to the unique chemistry that is not observed on either Pt or C/W(111) alone. Upon the adsorption of methanol on Pt/C/W(111), the uncovered portion of the C/W(111) surface dissociates the O–H bond of methanol to produce surface methoxy. Subsequently, the submonolayer Pt reacts with the C–H bonds of methoxy, which would be responsible for the dissociation of methoxy at temperatures that are lower than those on C/W(111), as compared in Figs. 5–8. In addition, the facile C–H bond cleavage on Pt/C/W(111) would be responsible for the absence of the methane gas-phase product from the dissociation of methoxy, as confirmed in Fig. 2. Overall, the resulting synergistic effect on submonolayer Pt/C/W(111) could potentially have important impact in the application of carbide-based catalysts in fuel cells as well as in other hydrocarbon transformation reactions.

5. Conclusions

On C/W(111), methanol molecules decompose to CO, H_2, CH_4, atomic carbon, and atomic oxygen by three pathways. In contrast, on Pt-modified C/W(111) surfaces, methanol molecules decompose to CO, atomic carbon, atomic oxygen, and H_2 without producing the undesirable by-product CH_4. For example, on the 0.6 ML Pt/C/W(111) surface, $\sim$ 49% of methanol molecules decompose to CO and hydrogen directly and the other $\sim$ 51% methanol molecules decompose to atomic carbon, atomic oxygen, and H_2. Such comparison clearly demonstrates a synergistic effect of Pt/C/W(111) surfaces in the dissociation of methanol. Furthermore, both C/W(111) and 0.6 ML Pt/C/W(111) surfaces remain active toward the dissociation of water and hydrogen. Overall these results illustrate the feasibility of using Pt-modified tungsten carbides as potential electrocatalysts in direct methanol or hydrogen fuel cells.

Acknowledgments

We acknowledge financial support from the Basic Energy Sciences, Department of Energy (DOE/BES Grant DE-FG02-00ER15014). We also acknowledge partial support from DuPont and the Delaware Research Partnership. We also thank Henry Hwu and Brian Polizzotti for assistance with experiments.

References

[1] G.J.K. Acres, J.C. Frost, G.A. Hards, R.J. Potter, T.R. Ralph, D. Thompsett, G.T. Burstein, G.J. Hutchings, Catal. Today 38 (1997) 393.
[2] M.M.P. Janssen, J. Moolhuysen, Electrochim. Acta 21 (1976) 869.
[3] M.M.P. Janssen, J. Moolhuysen, Electrochim. Acta 21 (1976) 861; J. Catal. 46 (1977) 289.
[4] K. Wang, H.A. Gasteiger, N.M. Markovic, P.N. Ross Jr., Electrochim. Acta 41 (1996) 2587.
[5] K.J. Cathro, J. Electrochem. Soc. 116 (1969) 1608.
[6] S. Szabo, J. Electroanalyst. Chem. 172 (1969) 359.
[7] S. Gilman, M.W. Breiter, J. Electrochem. Soc. 109 (1962) 1099.
[8] A.N. Haner, P.N. Ross, J. Phys. Chem. 95 (1991) 3740.
[9] S.A. Campbell, R. Parsons, J. Chem. Soc. Faraday Trans. 88 (6) (1992) 833.
[10] C. Panja, N. Saliba, B.E. Koel, Surf. Sci. 395 (1998) 248, and references therein.
[11] S.T. Oyama, The Chemistry of Transition Metal Carbides and Nitrides, Blackie, Glasgow, 1996.
[12] J.G. Chen, Chem. Rev. 96 (1996) 1477, and references therein.
[13] J.G. Chen, M.D. Weisel, Z.M. Liu, J.M. White, J. Am. Chem. Soc. 115 (1993) 8875.
[14] B. Fruhberger, J.G. Chen, J. Am. Chem. Soc. 118 (1996) 11599.
[15] B. Fruhberger, J.G. Chen, Surf. Sci. 342 (1995) 38.
[16] J. Eng Jr., B.E. Bent, B. Fruhberger, J.G. Chen, J. Phys. Chem. B 101 (1997) 4404.
[17] J. Eng Jr., J.G. Chen, Surf. Sci. 414 (1998) 374.
[18] J.G. Chen, B. Fruhberger, Surf. Sci. 367 (1996) L102.
[19] J. Eng Jr., B.E. Bent, B. Fruhberger, J.G. Chen, Langmuir 14 (1998) 1301.
[20] N. Liu, S.A. Rykov, H.H. Hwu, M.T. Buelow, J.G. Chen, J. Phys. Chem. B. 105 (2001) 3894.
[21] N. Liu, S.A. Rykov, J.G. Chen, Surf. Sci. 487 (2001) 107.
[22] H.H. Hwu, J.G. Chen, K. Kourtakis, J.G. Lavin, J. Phys. Chem. B 105 (2001) 10037.
[23] H.H. Hwu, B.D. Polizzotti, J.G. Chen, J. Phys. Chem. B 105 (2001) 10051.
[24] S. Hantzer, M.S. Touvelle, J.G. Chen, US Patent 5,811,624.
[25] N. Liu, J.G. Chen, Catal. Lett. 77 (2001) 35.
[26] K.D. Childs, B.A. Carlson, L.A. LaVanier, J.F. Moulder, D.F. Paul, W.F. Stickle, D.G. Watson, Handbook of Auger Electron Spectroscopy, 3rd ed., Physical Electronics, 1995.
[27] C.Z. Dong, S.M. Shivaprasad, K.-J. Song, T.E. Madey, J. Chem. Phys. 99 (1993) 9172.
[28] T.E. Madey, K.-J. Song, C.-Z. Dong, R.A. Demmin, Surf. Sci. 247 (1991) 175.
[29] K. Pelhos, J.B. Hannon, G.L. Kellogg, T.E. Madey, Surf. Sci. 432 (1999) 115.
[30] M. Falk, E. Wharlley, J. Chem. Phys. 34 (1961) 1554.
[31] J.G. Chen, P. Basu, L. Ng, J.T. Yates Jr., Surf. Sci. 194 (1988) 397.
[32] F. Franks, Water: a Comprehensive Treatise, Vol. 1, Plenum, New York, 1972.
[33] B.A. Sexton, K.D. Rendulic, A.E. Hughes, Surf. Sci. 121 (1982) 181.
[34] K.D. Gibson, L.H. Dubois, Surf. Sci. 223 (1990) 59.
[35] B.A. Sexton, Surf. Sci. 102 (1981) 271.
[36] S. Akhter, J.M. White, Surf. Sci. 167 (1986) 101.
[37] B.A. Sexton, K.D. Rendulic, A.E. Hughes, Surf. Sci. 121 (1982) 181.
[38] C. Lamy, J.M. Leger, J. Clavilier, R. Parsons, J. Electroanal. Chem. 150 (1983) 71.
[39] N. Kizhakevariam, E.M. Stuve, Surf. Sci. 286 (1993) 246, and references therein.
[40] J.L. Davis, M.A. Barteau, Surf. Sci. 187 (1987) 387.
[41] J. Wang, R.I. Masel, Surf. Sci. 167 (1986) 101.
[42] M. Rebholz, N. Kruse, J. Chem. Phys. 95 (1991) 7745.
[43] P.A. Thiel, T.E. Madey, Surf. Sci. Rep. 7 (1987) 211.
[44] H. Ibach, S. Lehwald, Surf. Sci. 91 (1980) 187.
[45] B.A. Sexton, Surf. Sci. 94 (1980) 435.
[46] E. Langenbach, A. Spitzer, H. Lüth, Surf. Sci. 147 (1984) 179.
[47] N.D. Shinn, Surf. Sci. 278 (1992) 157.
[48] H.H. Hwu, J.G. Chen, submitted for publication.
[49] H.H. Hwu, J.G. Chen, J. Phys. Chem. B, in press.
[50] B.E. Bent, Chem. Rev. 96 (1996) 1361.